PKA and GAB2 play central roles in the FSH signaling pathway to PI3K and AKT in ovarian granulosa cells

Mary E. Hunzicker-Dunn[a,1], Blanca Lopez-Biladeau[a], Nathan C. Law[a], Sarah E. Fiedler[b], Daniel W. Carr[b], and Evelyn T. Maizels[c,2]

[a]School of Molecular Biosciences, Washington State University, Pullman, WA 99164; [b]Portland Veterans Affairs Medical Center, Oregon Health and Science University, Portland, OR 97239; and [c]Department of Cell and Molecular Biology, Northwestern University Feinberg School of Medicine, Chicago, IL 60611

Edited* by Lutz Birnbaumer, National Institute of Environmental Health Sciences, Research Triangle Park, NC, and approved September 13, 2012 (received for review April 3, 2012)

Controlled maturation of ovarian follicles is necessary for fertility. Follicles are restrained at an immature stage until stimulated by FSH secreted by pituitary gonadotropes. FSH acts on granulosa cells within the immature follicle to inhibit apoptosis, promote proliferation, stimulate production of steroid and protein hormones, and induce ligand receptors and signaling intermediates. The phosphoinositide 3-kinase (PI3K)/AKT (protein kinase B) pathway is a pivotal signaling corridor necessary for transducing the FSH signal. We report that protein kinase A (PKA) mediates the actions of FSH by signaling through multiple targets to activate PI3K/AKT. PKA uses a route that promotes phosphorylation of insulin receptor substrate-1 (IRS-1) on Tyr^{989}, a canonical binding site for the 85-kDa regulatory subunit of PI3K that allosterically activates the catalytic subunit. PI3K activation leads to activation of AKT through phosphorylation of AKT on Thr^{308} and Ser^{473}. The adaptor growth factor receptor bound protein 2-associated binding protein 2 (GAB2) is present in a preformed complex with PI3K heterodimer and IRS-1, it is an A-kinase anchoring protein that binds the type I regulatory subunit of PKA, and it is phosphorylated by PKA on Ser^{159}. Overexpression of GAB2 enhances FSH-stimulated AKT phosphorylation. GAB2, thus, seems to coordinate signals from the FSH-stimulated rise in cAMP that leads to activation of PI3K/AKT. The ability of PKA to commandeer IRS-1 and GAB2, adaptors that normally integrate receptor/nonreceptor tyrosine kinase signaling into PI3K/AKT, reveals a previously unrecognized route for PKA to activate a pathway that promotes proliferation, inhibits apoptosis, enhances translation, and initiates differentiation of granulosa cells.

Fertility in females requires controlled maturation of the oocyte and supporting theca and granulosa cells (GCs) that comprise the ovarian follicle. Follicles are restrained at the preantral stage until they are stimulated by FSH synthesized and secreted from pituitary gonadotropes. FSH directs GCs to proliferate and produce steroid hormones, such as estrogen and progesterone, protein hormones, including inhibin, and growth factors, such as VEGF. These hormones and growth factors not only regulate oocyte maturation and support the growth and differentiation of follicles but also regulate uterine receptivity and provide feedback to the hypothalamus and pituitary (reviewed in ref. 1). In response to FSH, follicles develop to a mature preovulatory stage competent to receive the surge of luteinizing hormone (LH) that promotes ovulation and terminal differentiation of GCs and theca cells to luteal cells.

FSH signals through its surface G protein-coupled receptor (GPCR) localized to GCs (2). A crucial pathway by which FSH signals is the PI3K pathway that leads to the phosphorylation and activation of the nodal kinase AKT (protein kinase B). Studies using dominant negative and constitutively active AKT showed that the AKT pathway is necessary but not sufficient for activation of many key FSH target genes, including the *LH receptor*, *3β-hydroxysteroid dehydrogenase*, *aromatase*, and *inhibin-a* (3). AKT targets in GCs include tuberin (4), forkhead box O factor 1 (FOXO1) (5–7), and FOXO3a (8). Phosphorylation and inactivation of tuberin enhances signaling through mammalian target of rapamycin complex 1 (mTORC1)/regulatory-associated protein of mTOR to enhance translation of several proteins in GCs, including the transcriptional activator hypoxia inducible factor-1α (HIF-1α) (4). Heterodimeric HIF-1, composed of HIF-1α and constitutively expressed HIF-1β, is necessary for induction of VEGF in GCs and seems to contribute to induction of the LH receptor and inhibin-α (4). AKT-stimulated phosphorylation of FOXO1 releases repressive actions of the transcriptional factor on a number of FSH target genes, including *cyclin D2*, *aromatase*, *epiregulin*, *P450scc*, and *inhibin-α* (5), as well as genes involved in the cholesterol biosynthetic pathway (9). AKT also signals to inhibit apoptosis, in part, by phosphorylation of FOXO3a to inhibit expression of the proapoptotic protein Bim-extra long (B-cell lymphoma-2 interacting modulator of cell death) (8).

PI3K is canonically activated on engagement of the insulin or insulin-like growth factor 1 (IGF_1) receptor tyrosine kinases (RTKs) (reviewed in refs. 10 and 11) (Fig. S1). With receptor activation, insulin receptor substrate (IRS) proteins bind to phosphorylated tyrosine (pTyr) residues (within the NPXY motif) on the RTK through specific pTyr binding domains (12). IRS proteins, in turn, are phosphorylated by RTKs on Tyr residues in the carboxyl terminus, creating binding sites for SRC homology-2 (SH2) domain-containing proteins such as PI3K and the adaptor growth factor receptor bound protein 2 (GRB2) (13). Activation of the heterodimeric PI3K, composed of an 85-kDa regulatory (R) subunit (p85) and a 110-kDa catalytic subunit (p110), occurs on binding of both SH2 domains contained within p85 (14) to dual phosphorylated (p)-YXXM motifs on IRS proteins. Active PI3K catalyzes the phosphorylation of phosphatidylinositol-4,5-bisphosphate to generate phosphatidylinositol-3,4,5-trisphosphate (PIP3). Increased levels of PIP3 at the plasma membrane facilitate proximate binding of both phosphoinositide-dependent kinase 1 and AKT through their pleckstrin homology domains, resulting in the phosphoinositide-dependent kinase 1-dependent phosphorylation of AKT on Thr^{308} in its activation loop. Full activation of AKT requires phosphorylation in the hydrophobic motif at Ser^{473} by mTORC2, which consists of mTOR complexed to rapamycin insensitive companion of mTOR and other proteins (reviewed in ref. 10).

Author contributions: M.E.H.-D., B.L.-B., N.C.L., S.E.F., D.W.C., and E.T.M. designed research; M.E.H.-D., B.L.-B., N.C.L., S.E.F., and E.T.M. performed research; M.E.H.-D., D.W.C., and E.T.M. analyzed data; and M.E.H.-D. wrote the paper.

The authors declare no conflict of interest.

*This Direct Submission article had a prearranged editor.

[1]To whom correspondence should be addressed. E-mail: mehd@wsu.edu.

[2]Present address: Biomedical Visualization Program, Department of Biomedical and Health Information Sciences, University of Illinois, Chicago, IL 60612.

See Author Summary on page 17742 (volume 109, number 44).

This article contains supporting information online at www.pnas.org/lookup/suppl/doi:10.1073/pnas.1205661109/-/DCSupplemental.

For other RTKs and cytokine receptors, PI3K is activated on binding to a member of the GRB2-associated binding protein (GAB) family of scaffold proteins that are functionally related to IRS proteins (reviewed in refs. 15 and 16). GABs link to these RTKs through GRB2 and are phosphorylated on a number of Tyr residues that create binding sites for PI3K and other signaling molecules (reviewed in ref. 17). PI3K can also be activated by binding of activated (GTP-bound) RAS to the RAS binding domain present on each of the p110 catalytic subunits (α, β, δ, and γ); however, the contribution of RAS to PI3K activation under physiological conditions is not clear (reviewed in ref. 18).

The mechanism by which GPCRs regulate PI3K activity is more diverse and less well-understood. Although GPCRs may activate PI3K through transactivation of RTKs, GPCRs more commonly activate p110 catalytic subunits through direct binding of $G_{\beta\gamma}$ subunits (reviewed in ref. 18). Alternatively, GPCRs may

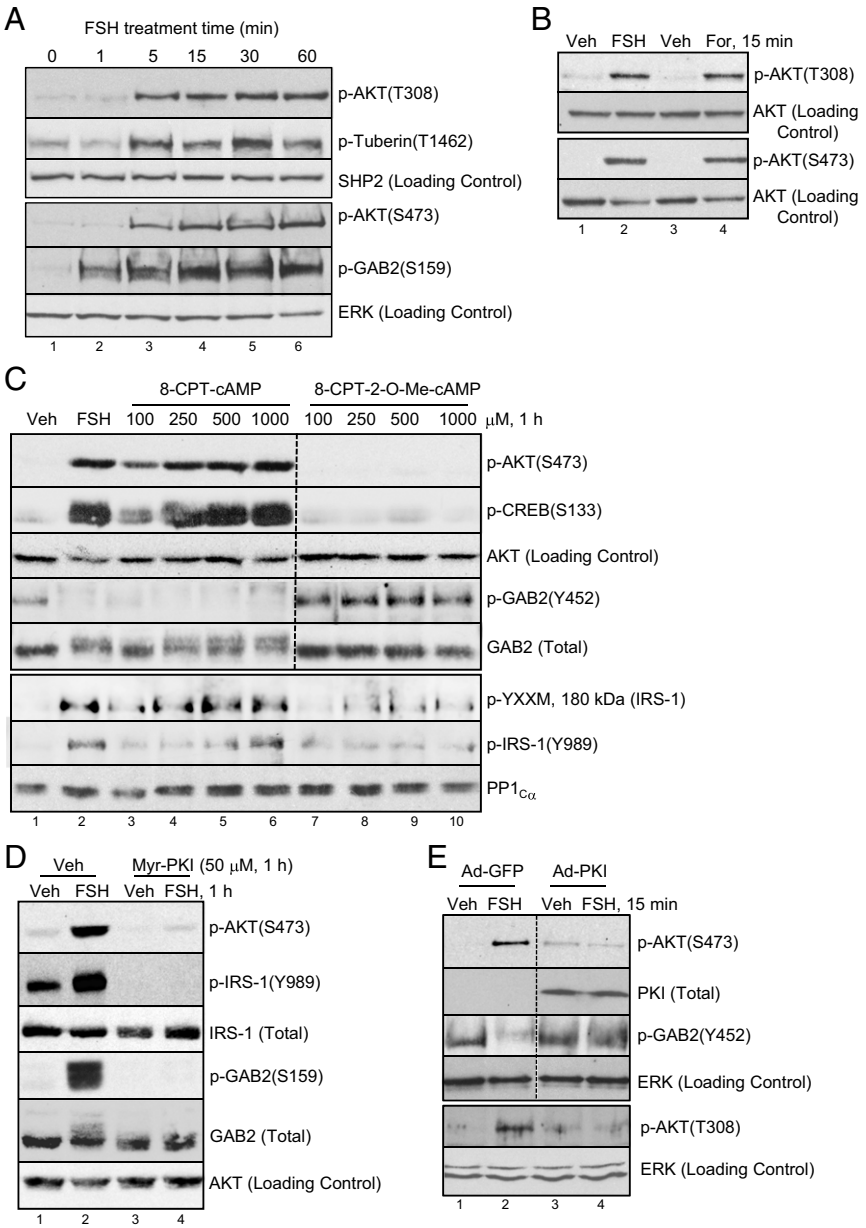

Fig. 1. FSH-stimulated phosphorylation of AKT on Thr^{308} and Ser^{473} is mediated by PKA. (*A*) GCs were treated for indicated times without (time 0) or with 50 ng/mL FSH. After heat denaturation in SDS sample buffer and SDS/PAGE, a blot of total cell extracts was sequentially probed with indicated antibodies. Separate panels reflect results with the same samples run on different gels (hence, distinct loading controls). Results are representative of three independent experiments. The rest of the conditions are described in *Materials and Methods*. (*B*) GCs were treated for 15 min with vehicle (DMEM; lane 1), FSH (lane 2), 0.25% ethanol/DMEM (lane 3), or 10 μM forskolin in 0.25% ethanol/DMEM (lane 4). The rest of the conditions are described in *A*. Results are representative of four independent experiments. (*C*) GCs were treated without or with FSH or with indicated concentrations of 8-CPT-cAMP or 8-CPT-2-O-Me-cAMP for 1 h. Dotted lines between lanes represent cropped images. Results are representative of four independent experiments. (*D*) GCs were pretreated with vehicle (water) or 50 μM Myr-PKI for 1 h followed by treatment without or with FSH for 1 h. FSH-stimulated phosphorylations of AKT(Ser^{473}), IRS-1(Tyr^{989}), and GAB2 (Ser^{159}) were inhibited by Myr-PKI [93.8 ± 2.4% (n = 4), 88.0 ± 10.8% (n = 2), and 95.3 ± 2.2% (n = 2), respectively]. (*E*) GCs were transduced overnight with Ad-GFP (5.8×10^3 OPU/cell) or PKI (1.8×10^4 OPU/cell) that expresses the full-length PKI protein. Cells were then treated 15 min without or with FSH. FSH-stimulated phosphorylations of AKT(Ser^{473}), GAB2(Tyr^{452}), and AKT (Thr^{308}) were inhibited by PKI [97.0 ± 2.3% (n = 5), 96.9 ± 3.2% (n = 4), and 100 ± 0% (n = 4), respectively]. The rest of the conditions are described in *A*.

activate PI3K recruited to GPCR-signaling complexes that contain adaptors, like β-arrestin, or G protein-regulated kinases; however, details of the molecular mechanisms are incomplete (reviewed in ref. 18). GPCRs that signal through PKA are reported to phosphorylate the p85 R-subunit, enhancing RAS binding and activation of p110 catalytic activity (19–21).

Here, we show that both GAB2 and IRS-1 adaptors are appropriated by PKA to activate the PI3K pathway in GCs, resulting in the phosphorylation of IRS-1 on Tyr^{989}, a canonical p-YXXM binding site for the p85 R-subunit of PI3K, and consequent phosphorylation of AKT on Thr^{308} and Ser^{473}. GAB2 seems to play a central role in the mechanism by which FSH signals to activate PI3K/AKT; overexpression of GAB2 enhances FSH-stimulated AKT phosphorylation. GCs exhibit a preformed complex consisting of GAB2, the PI3K heterodimer, and IRS-1. GAB2 directly binds the type I regulatory subunit (RI) of PKA, anchoring PKA to this complex. FSH through PKA indirectly promotes the dephosphorylation of GAB2(Tyr^{452}) and phosphorylation of IRS-1(Tyr^{989}), and it directly phosphorylates GAB2 on Ser^{159}. The ability of PKA to hijack the pathway that promotes cellular proliferation, inhibits apoptosis, enhances translation, and initiates differentiation reveals an FSH signaling mechanism in GCs that supports cell survival, proliferation, and differentiation.

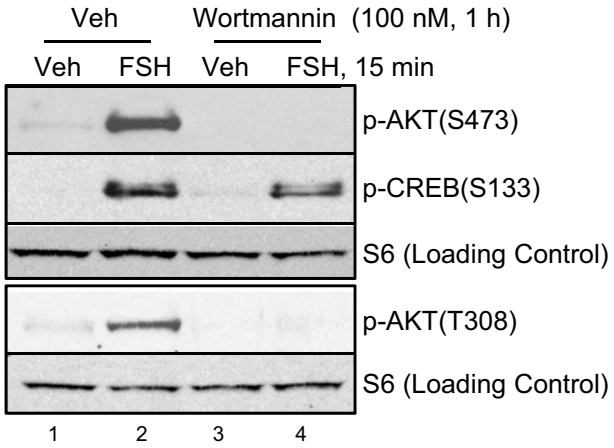

Fig. 2. The PI3K inhibitor wortmannin blocks FSH-stimulated phosphorylations of AKT(Ser^{308}) and (Thr^{473}). GCs were pretreated with vehicle (DMSO) or 100 nM wortmannin for 1 h and then treated without or with FSH for 15 min. FSH-stimulated phosphorylations of AKT(Ser^{473}), CREB(Ser^{133}), and AKT(Thr^{308}) were inhibited [98.1 ± 2.2% (n = 4), 5.2 ± 2.9% (n = 3), and 96.6 ± 2.5% (n = 3), respectively] by wortmannin. The rest of the conditions are described in Fig. 1*A*.

Results

FSH Signals to Promote Activation of AKT Through a PKA-Dependent Pathway. FSH enhances the phosphorylation of AKT on both the proximal Thr^{308} and distal Ser^{473} sites and the downstream target tuberin on Thr^{1462} within 5 min of treatment (Fig. 1*A*). Enhanced AKT(Thr^{308})(Ser^{473}) phosphorylations are mimicked by the adenylyl cyclase activator forskolin (Fig. 1*B*). AKT(Ser^{473}) phosphorylation is also stimulated by 8-chlorophenylthiol (CPT) -cAMP, the cell permeable cAMP analog that activates both PKA and exchange proteins activated by cAMP (22, 23), but it is not stimulated by the cAMP analog 8-CPT-2-O-Me-cAMP that does not activate PKA (24) (Fig. 1*C*). Phosphorylation of cAMP response element binding protein (CREB) (Ser^{133}) serves as a positive control (Fig. 1*C*). Consistent with a mediatory role for PKA in the activation of AKT, pretreatment of GCs with myristoylated (Myr) -PK inhibitor (PKI) peptide, which functions as a pseudosubstrate for the catalytic subunit of PKA (25), or adenoviral-PKI, which expresses the full-length PKI protein, abrogates FSH-stimulated AKT(Thr^{308})(Ser^{473}) phosphorylations (Fig. 1 *D* and *E*) [100 ± 0% (n = 4) and 97 ± 2.3% inhibition (n = 5), respectively; full statistics in legend]. The ability of the PI3K inhibitor wortmannin (26) to prevent FSH-stimulated AKT(Thr^{308}) (Ser^{473}) phosphorylations (Fig. 2) [96.6 ± 2.5% (n = 3) and 98.1 ± 2.2% (n = 4) inhibition, respectively] supports the expectation that PI3K is upstream of AKT in GCs. Wortmannin does not inhibit canonical PKA signaling to CREB(Ser^{133}) (Fig. 2) [5.2 ± 2.9% (n = 3)], a direct PKA target (27) in GCs (28). Taken together, these results show that FSH signals by kinases activated by the PI3K product PIP3 (10) to promote AKT(Thr^{308})(Ser^{473}) phosphorylations through a PKA-dependent mechanism.

FSH Promotes the PKA-Dependent Phosphorylation of IRS-1(Tyr^{989}). PKA is reported in thyroid and vascular smooth muscle cells to phosphorylate the p85 R-subunit of PI3K on Ser^{83}, enhancing RAS binding to and activation of p110 (19–21). To test whether p85 is a PKA target in GCs, after treatment of GCs with vehicle or FSH, we used an agarose-conjugated anti-p85 antibody vs. control agarose-conjugated IgG for immunoprecipitation and probed blots with a p-PKA substrate ($RRXS^P/T^P$) antibody. Although the p-PKA substrate antibody detected prominent phosphorylations in FSH-treated GCs (Fig. S2*A*, lanes 2 and 4), no signal was detected at 85 kDa with p85 R-subunit immunoprecipitation (lane 8), despite the ability of the anti-p85 antibody to deplete p85 (Fig. S2*B*). Transduction of GCs with a dominant negative (S17N) -RAS did not strongly compromise FSH-stimulated AKT(Thr^{308})(Ser^{473}) phosphorylations but prevented the phosphorylation of ERK (Fig. S2*C*). These results suggest that PI3K in GCs is activated by a PKA-dependent pathway distinct from that reported in thyroid and vascular smooth muscle cells.

Considering the canonical mechanism for PI3K activation, we sought to determine in GCs if a Tyr-phosphorylated protein(s) bound the p85 R-subunit of PI3K [rat GCs express p85β(Pik3r2), p55γ(Pik3r3), p150(Pik3r4) (predicted), p110α(Pik3ca) (predicted), p110β(Pik3cb), p110δ(Pik3cd) (predicted), and p110γ (Pik3cg) but do not express detectable levels of p85α(Pik3r1), p101(Pik3r5), and p87(Pik3r6) class I PI3K subunit isoforms (29)]. To this end, we used an antibody that detects the binding motif (p-YXXM) recognized by the SH2 domain of the PI3K p85 R-subunit (12) to probe total cell extracts from GCs treated with vehicle, FSH, or a positive control, IGF_1. Results (Fig. 3*A* and Fig. S3) show that a single band ∼80 kDa from vehicle-treated GCs exhibits the pTyr p85 binding motif (Fig. 3*A*, lane 1, top section). Treatment with FSH or IGF_1 promotes the appearance of a protein band ∼185 kDa that exhibits the pTyr p85 binding motif concomitant with the disappearance of the p85 binding motif signal ∼80 kDa (Fig. 3*A*, lanes 2 and 3 compared with lane 1, top section).

We identified the ∼80-kDa protein that contains the p-YXXM motif in vehicle-treated GCs as GAB2 (Fig. 3*A*) (GAB1 in GCs migrates on SDS/PAGE ∼100 kDa and does not exhibit the molecular weight shift in FSH-treated GCs that GAB2 exhibits). GAB2 is phosphorylated on Tyr^{452} [Y^{441}VPM (homologous rat sequence)] in vehicle-treated cells (Fig. 3*A*, lane 1). Overexpression of WT GAB2 (2.8 ± 1.0-fold, n = 3) from an adenoviral vector promotes elevated p-YXXM signal at 80 kDa (Fig. 3*B*, lane 3) (193.0 ± 73.5%, n = 3, $P < 0.05$) compared with empty vector (lane 1). This phosphorylation signal disappears on treatment of cells with FSH (Fig. 3 *A*, lane 2, and *B*, lanes 2 and 4) or IGF_1 (Fig. 3*A*, lane 3). This result suggests that the p85 R-subunit of PI3K may bind GAB2 at Tyr^{452} in the absence of FSH or IGF_1 signals and that this association is terminated on dephosphorylation of GAB2 by FSH- or IGF_1-dependent mechanisms. Overexpression of WT GAB2 also modestly but significantly enhances AKT(Ser^{473}) phosphorylation (Fig. 3*B*) (82.7 ± 36.3%, n = 3, $P < 0.05$). This result suggests that GAB2,

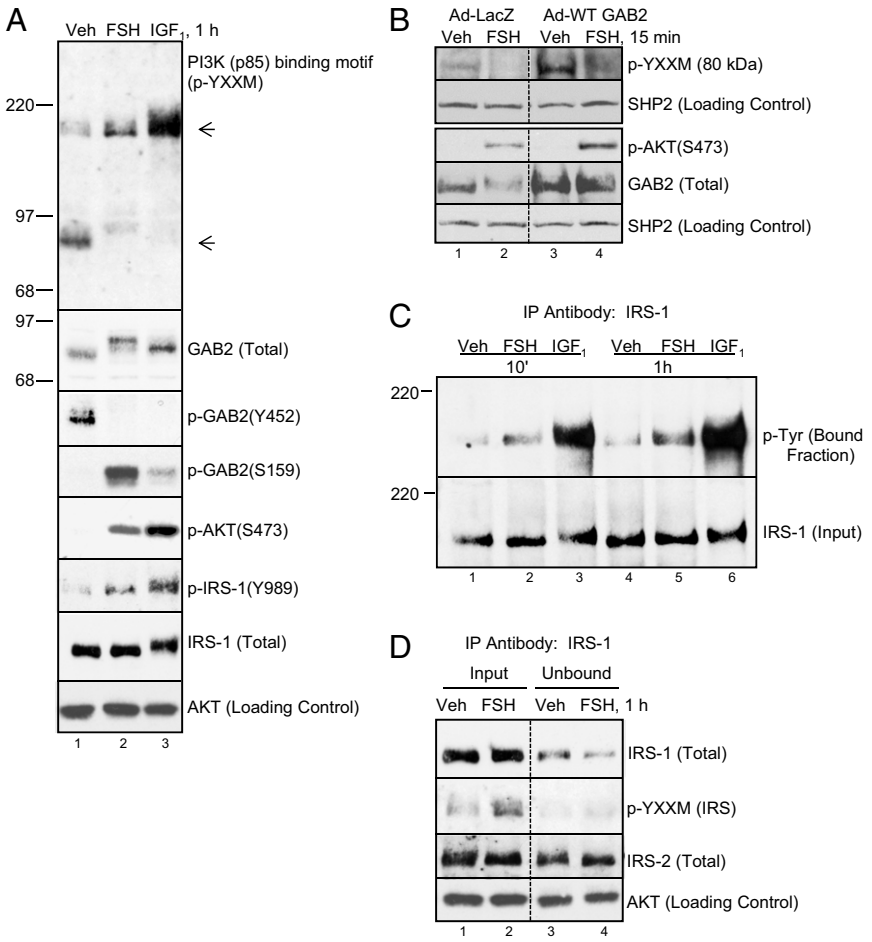

Fig. 3. FSH regulates the phosphorylation of YXXM binding motifs for p85 R-subunit on both GAB2 and IRS-1. (*A*) GCs were treated without or with FSH or 50 ng/mL IGF_1 for 1 h. Blot of total cell extracts was probed with indicated antibodies. Molecular weight markers are shown only for binding motif and total GAB2, and the latter shows a characteristic upshift that is, in part, attributable to phosphorylation on Ser^{159}. Results are representative of two independent experiments. Equivalent results for vehicle and FSH treatments were seen in three additional experiments. Full p-YXXM blot is show in Fig. S3. (*B*) GCs were transduced overnight with Ad-LacZ (1.6×10^5 OPU/cell) or WT GAB2 (5.4×10^5 OPU/cell). Cells were then treated for 15 min without or with FSH and probed for indicated antibodies. The rest of conditions are described in Fig. 1*A*. Results are representative of three independent experiments. (*C*) GCs were treated with vehicle, FSH, or IGF_1 for 10 min or 1 h. Cells were scraped into lysis buffer and sonicated, and insoluble particulate was removed by centrifugation. Soluble extracts were incubated with anti–IRS-1 agarose-conjugated antibody. Immunoprecipitated (bound) and input fractions were probed with indicated antibodies. Results are representative of three independent experiments. (*D*) GCs were treated without or with FSH for 1 h. Soluble extracts were subjected to immunoprecipitation with anti–IRS-1 agarose-conjugated antibody, which was described in *B*. Input and unbound (flow-through) fractions were probed with indicated antibodies. Results are representative of two independent experiments.

indeed, participates in the FSH signaling pathway that leads to AKT activation. GAB2 is also phosphorylated on Ser^{159} in response to FSH and to a lesser extent, IGF_1 (Fig. 3*A*).

The ~185-kDa protein band that exhibits the pTyr p85 binding motif in FSH- and IGF_1-treated GCs corresponds to IRS-1. This conclusion is based, in part, on FSH- and IGF_1-stimulated phosphorylation of IRS-1(Tyr^{989}) (Fig. 3*A*), a p-Y^{987}MTM (homologous rat sequence) motif (13). Tyr phosphorylation of IRS-1 was also detected with immunoprecipitation of IRS-1 from cells treated with FSH and IGF_1 on blots probed with a pan p-Tyr antibody (Fig. 3*C*). Because both IRS-1 and IRS-2 migrate on SDS/PAGE at the same molecular mass, we evaluated the ability of the IRS-1 antibody to deplete p-YXXM signal in an immunoprecipitation experiment. Results (Fig. 3*D*) show that immunoprecipitation with anti–IRS-1 antibody depletes the majority (84.6 ± 5.2%) of the p-YXXM signal in FSH-treated GCs. These results suggest that, in response to FSH, the p85 R-subunit of PI3K binds predominately to IRS-1.

FSH-stimulated phosphorylation of IRS-1(Tyr^{989}) and dephosphorylation of GAB2(Tyr^{452}) are mimicked by 8-CPT-cAMP and blocked by Myr-PKI and Ad-PKI (Fig. 1 *C–E*) [88 ± 10.8% (n = 2) and 96.9 ± 3.2% (n = 3) inhibition, respectively]. Phosphorylation of GAB2(Ser^{159}) is also inhibited by Myr-PKI (Fig. 1*D*) [95.3 ± 2.2% (n = 2)]. These results suggest that the phosphorylation status of the p-YXXM motifs on both GAB2 and IRS-1 and the phosphorylation status of Ser^{159} on GAB2 are regulated by PKA.

GAB2 Signalsome. Because FSH promotes dephosphorylation of a p-YXXM motif on the adaptor protein GAB2, we investigated whether GAB2 complexes with PI3K and IRS-1 in GCs. To this end, GC extracts were subjected to immunoprecipitation with anti-GAB2 antibody vs. control IgG, and blots were probed for the p85 R-subunit of PI3K and IRS-1. Results (Fig. 4*A*) show that GAB2 complexes selectively with both the p85 R-subunit of PI3K and IRS-1. Although this complex forms independently of FSH, FSH promotes a modest loss of IRS-1 from the GAB2 signaling complex (30.4 ± 4.6%, n = 4). The anti-GAB2 antibody depletes GC extracts of >90% of GAB2 (Fig. S4*A*); however, a minor fraction of total p85 R and IRS-1 is immunoprecipitated

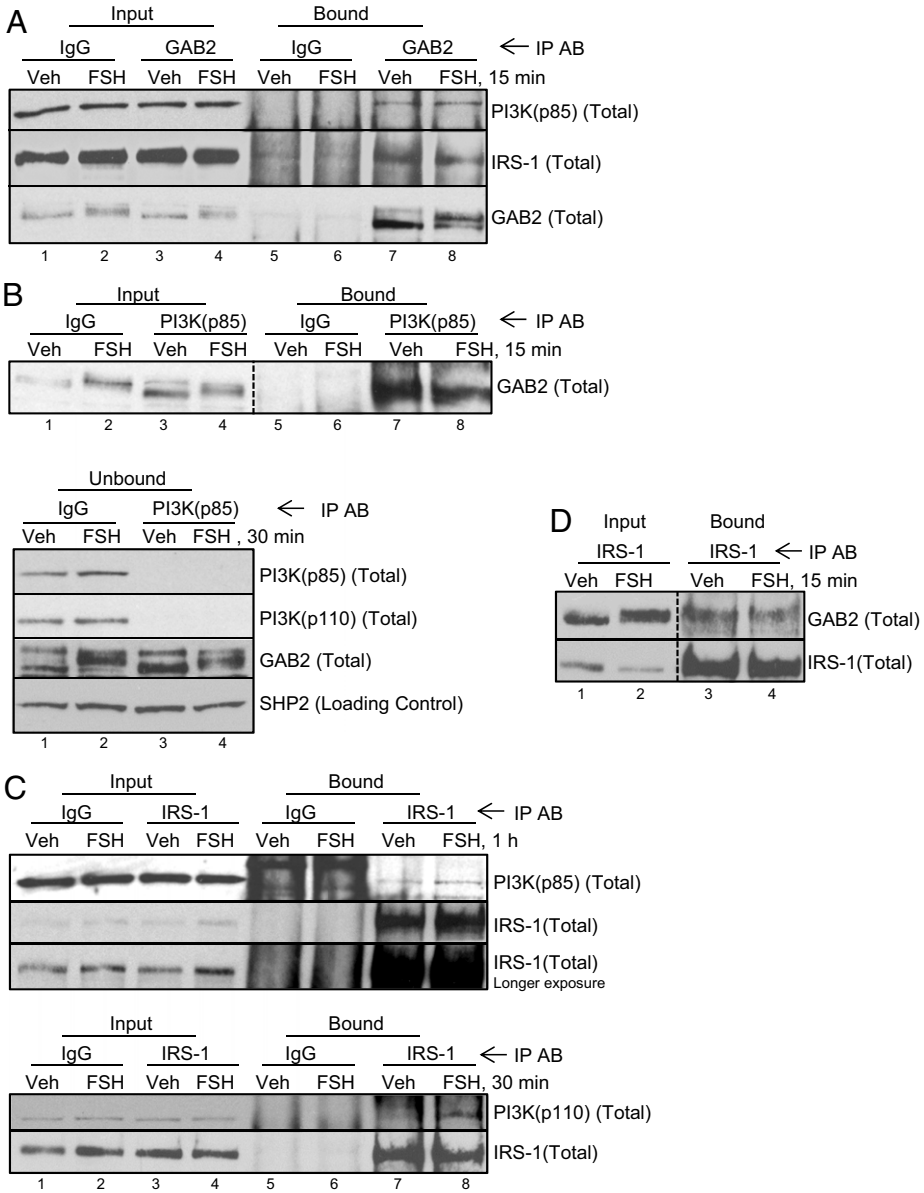

Fig. 4. GAB2, IRS-1, and PI3K are present in GCs in a preformed complex. (*A*) GCs were treated without or with FSH for 15 min, scraped into lysis buffer, and sonicated, and particulate was removed by centrifugation. After taking corresponding input aliquots, soluble extracts were precleared and incubated with control IgG or anti-GAB2 antibody overnight in the presence of protein A/G PLUS agarose. Blots of input (3% of total sample) and proteins bound to washed agarose beads (immunoprecipitated; 97% of total sample) were probed with indicated antibodies. Results are representative of three independent experiments. Depletion of GAB2 in unbound fractions (>90%) from a separate experiment is shown in Fig. S4*A*. (*B*) GCs were treated without or with FSH for 15 min; soluble precleared extracts were subjected to immunoprecipitation with IgG or anti–p85-PI3K agarose-conjugated antibodies. Results are representative of three independent experiments. In *Lower*, unbound fractions from a separate experiment were probed with indicated antibodies. (*C*) GCs were treated without or with FSH for 1 h or 30 min (*Lower*); soluble precleared extracts were subjected to immunoprecipitation with IgG or anti–IRS-1 agarose–conjugated antibodies. Results are representative of two independent experiments. Depletion of IRS-1 in unbound fractions (~80%) is shown in Fig. S4*B*. (*D*) GCs were treated without or with FSH for 15 min; soluble precleared extracts were subjected to immunoprecipitation with anti–IRS-1 agarose–conjugated antibodies. Results are representative of 10 independent experiments.

based on the presence of equivalent levels of signal in unbound fractions. Immunoprecipitation with the anti-p85 antibody–agarose conjugate selectively pulls down equivalent levels of GAB2 in vehicle- and FSH-treated GCs (Fig. 4*B*) (relative to input, $P > 0.05$). This antibody depletes GC extracts of both the p85 and p110 PI3K subunits independent of FSH treatment, consistent with the presence of a functional PI3K heterodimer, but it pulls down a relatively minor fraction of total GAB2 (Fig. 4*B*, *Lower*). Likewise, immunoprecipitation with anti–IRS-1 antibody–agarose conjugate selectively pulls down p85 R- and p110 catalytic subunits of PI3K preferentially from FSH-treated GCs (Fig. 4*C*). This antibody depletes extracts of ~80% of IRS-1 but pulls down a minimal fraction of total p85 (Fig. S4*B*). Immunoprecipitation with anti–IRS-1 antibody–agarose conjugate also selectively pulls down GAB2 from vehicle-treated GCs (Fig. 4*D*, lane 3); this IRS-1/GAB2 association is moderately compromised in cells treated with FSH (28.9 ± 9.1% decrease, $n = 10$, $P < 0.05$) [treatment of GCs with FSH (15 min to 1 h) does not significantly reduce total levels of GAB2 compared with vehicle controls quantified on Western blots relative to loading controls (1.06 ± 0.05, $n = 21$).

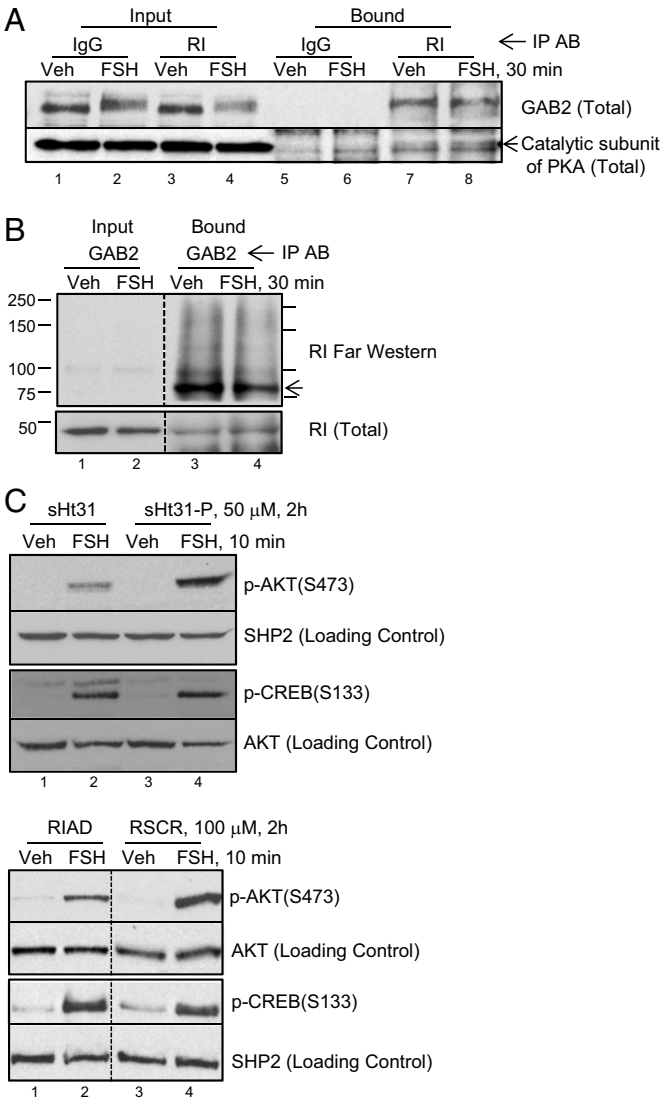

Fig. 5. GAB2 is an RI AKAP. (*A*) GCs were treated without or with FSH for 30 min; soluble precleared lysates were subjected to immunoprecipitation with IgG or anti-RI antibody. Results are representative of two independent experiments. (*B*) GCs were treated without or with FSH for 30 min; soluble precleared lysates were subjected to immunoprecipitation with anti-GAB2 antibody. Proteins separated by PAGE were transferred to PVDF membrane. The top portion of the membrane was incubated with purified RIα, which was described in *Materials and Methods*, and then, it was subjected to RI Western blotting; the lower portion of the membrane was subjected directly to RI Western blotting. The arrow marks the migration position for GAB2. Results for the RI far Western assay are representative of seven independent experiments; results of the RI Western assay are representative of five independent experiments. (*C*) GCs were pretreated for 2 h with 50 μM sHt31 or sHt31-P or 100 μM RIAD or RSCR, and then, they were treated without or with FSH for 10 min. The rest of the conditions are described in Fig. 1*A*. Results are representative of two and three independent experiments, respectively.

Taken together, these results suggest that a preformed complex consisting of GAB2, p85/p110 PI3K subunits, and IRS-1 exists in GCs. Although these associations are specific, they do not seem to be stoichiometric relative to the amount of protein pulled down by immunoprecipitating antibody. However, we cannot rule out the potentially adverse effects of cellular disruption and overnight immunoprecipitation on the stoichiometry of this complex.

Inasmuch as the phosphorylation of IRS-1 and dephosphorylation of GAB2 on p-YXXM motifs are dependent on PKA, we asked if the GAB2 signaling complex also contained PKA. Based on the abundance of the RI in preantral GCs (30), we tested if RI coimmunoprecipitates with GAB2. Results show that anti-RI antibody selectively pulls down GAB2 and the catalytic subunit of PKA (Fig. 5*A*) and that anti-GAB2 antibody pulls down RI (Fig. 5*B*, *Lower* and Fig. S5, *Bottom*). We then tested whether GAB2 binds directly to RI using a far Western approach. RI, indeed, binds directly (Fig. 5*B*, *Upper*, lanes 3 and 4) and selectively (Fig. S5, *Top*, lanes 7 and 8) to immunoprecipitated GAB2. RI binding to GAB2 in vitro is displaced by the competitive amphipathic helix peptide Ht31 (Fig. S5, *Middle*), and RI binding to GAB2 is not significantly different between vehicle- and FSH-treated GCs ($P > 0.05$, $n = 6$). GAB2 does not seem to directly bind the type II PKA R-subunit based on a type II PKA R-subunit (RII) overlay assay (Fig. S6*A*), whereas RII bound selectively to the positive control microtubule-associated protein 2D and an unidentified ~30-kDa protein in GC extracts (Fig. S6*B*). These results suggest that GAB2 is a selective RI A-kinase anchoring protein (AKAP). Consistent with this conclusion, competitive displacement of PKA from AKAPs by stearated (s)Ht31 compared with inactive sHt31-P (31) or the selective RI anchoring disruptor (RIAD) compared with a scrambled RIAD peptide (RSCR) (32) reduced AKT(Ser^{473}) phosphorylation (63.2 ± 11.6% and 32.5 ± 7.5%, respectively) but did not significantly ($P > 0.05$) disrupt CREB(S^{133}) phosphorylation (14.9 ± 10.5% and 11.5 ± 11.5%, respectively) (Fig. 5*C*).

Because GAB2 is also phosphorylated on Ser^{159} in a PKA-dependent manner (Fig. 1*D*), we asked whether GAB2 is a direct PKA target. Ser^{159} on GAB2, corresponding to $RKSS^{160}$ of rat GAB2, matches the PKA consensus phosphorylation motif RR/KXS^{P}/T^{P} (33). GAB2 is selectively immunoprecipitated using an anti–p-PKA substrate antibody that recognizes an $RXXS^{P}/T^{P}$ motif (Fig. 6*A*) and is phosphorylated in an immune complex phosphorylation reaction in the presence of the catalytic subunit of PKA (Fig. 6*B*). Finally, the phosphorylation of GAB2(Ser^{159}) precedes the phosphorylation of AKT(Ser^{473}) (Fig. 6*C*). Together, these results indicate that GAB2 is a direct PKA target. We then asked whether GAB2, on phosphorylation on Ser^{159}, remains in complex with PKA, IRS-1, and PI3K. Results from immunoprecipitations using anti–p-GAB2(Ser^{159}) (Figs. 6*D* and Fig. S7*A*) show that the majority of GAB2 is phosphorylated on Ser^{159} in FSH-treated cells (76.0 ± 3.2%, $n = 3$) based on the ability of the p-GAB2(Ser^{159}) antibody to deplete total GAB2 from unbound fractions; anti–p-GAB2(Ser^{159}) readily pulls down IRS-1, but surprising, anti–p-GAB2(Ser^{159}) antibody does not pull down RI. Similarly, anti-RI antibody does not pull down p-GAB2(Ser^{159}) (Fig. S7*B*). Immunoprecipitation with anti-p85 antibody–agarose conjugate also pulls down p-GAB2(Ser^{159}) (Fig. 6*E*). Together, these results show that RI preferentially binds GAB2 that is not phosphorylated on Ser^{159} and that PKA promotes the dissociation of a complex that contains p-GAB2 (Ser^{159}), IRS-1, and the PI3K heterodimer.

Discussion

Our results reveal a mechanism by which FSH activates the PI3K pathway, leading to activation of AKT and downstream targets in GCs. As modeled in Fig. 7, FSH in a PKA-dependent manner stimulates the phosphorylation of GAB2 on Ser^{159}, dephosphorylation of GAB2 on Tyr^{452}, a p85 R-subunit binding site, and phosphorylation of IRS-1 on Tyr^{989}. Tyr^{989} on IRS-1 comprises one of two YXXM motifs on IRS-1, with phosphorylation that permits binding of the p85 R-subunit of PI3K (12), resulting in allosteric activation of the p110 catalytic subunit and consequent phosphorylation of AKT on both the proximal Thr^{308} and distal Ser^{473} sites to promote full AKT activation.

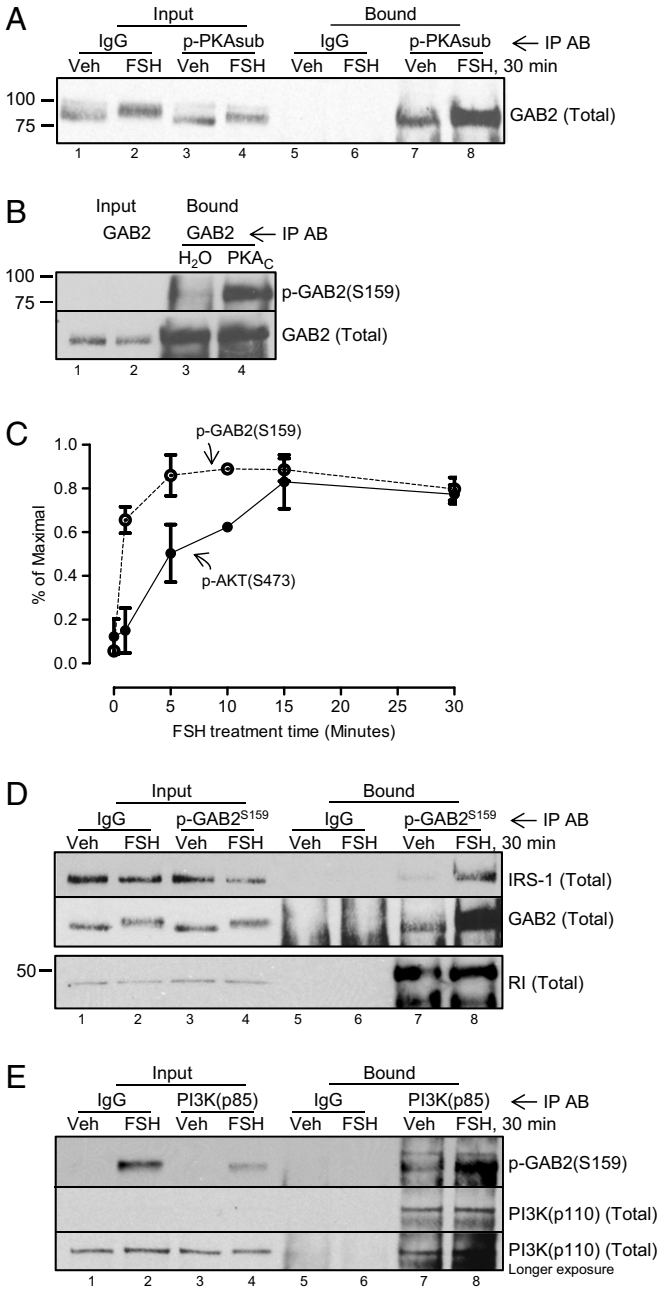

Fig. 6. GAB2 is phosphorylated on Ser^{159} by PKA. (*A*) GCs were treated without or with FSH for 30 min; soluble precleared lysates were subjected to immunoprecipitation with IgG or antiphospho-PKA substrate (p-PKAsub) antibody. Results are representative of two independent experiments. (*B*) Soluble precleared lysates from untreated GCs were subjected to immunoprecipitation with anti-GAB2 antibody. Washed immunoprecipitates were then subjected to an in vitro phosphorylation assay in the absence or presence of the catalytic subunit of PKA (PKA_C), which was described in *Materials and Methods*. Results are representative of three independent experiments. (*C*) Phosphorylations of GAB2(Ser^{159}) and AKT(Ser^{473}) (Fig. 1*A*) are plotted as a percent of the maximal signal (means ± SEMs; n = 3 for 1-, 5-, and 30-min points; n = 2 for 15-min point; n = 1 for 10-min point). (*D*) GCs were treated without or with FSH for 30 min; soluble precleared lysates were subjected to immunoprecipitation with IgG or anti-p-GAB2(Ser^{159}) antibody. Two independent experiments are shown. Results are representative of four independent experiments. (*E*) GCs were treated without or with FSH for 30 min; soluble precleared lysates were subjected to immunoprecipitation with IgG or anti-p85 R-subunit antibodies. Results are representative of three independent experiments.

Indeed, the only detectable FSH-stimulated p-YXXM signal in GCs migrates on SDS/PAGE at a molecular weight consistent with the molecular weight of IRS proteins (~185 kDa). FSH-stimulated IRS-1 phosphorylation is confirmed with both anti–p-IRS-1(Tyr^{989}) antibody and pan anti–p-Tyr antibody after IRS-1 immunoprecipitation. Although the majority of the p-YXXM signal seems to be associated with IRS-1, we cannot rule out a contribution from IRS-2. Female IRS-2 null mice are infertile; however, the major effect seems to be at the level of the pituitary (34).

In GCs, GAB2 seems to play a unique and potentially central role in the mechanism by which FSH signals through its GPCR and PKA to activate PI3K. This conclusion is based on coimmunoprecipitation of GAB2 and IRS-1, PKA-dependent regulation of the phosphorylation status of relevant PI3K binding sites on GAB2 and IRS-1 and phosphorylation of GAB2 on Ser^{159}, and the ability of overexpressed WT GAB2 to significantly enhance AKT (Ser^{473}) phosphorylation, albeit modestly. GAB1, -2, and -3 comprise a ubiquitous family of adaptor proteins that amplify signals from RTKs and cytokine receptors to various signaling pathways (17). They contain many sites for Ser/Thr and Tyr phosphorylation as well as an N-terminal pleckstrin homology domain and central proline-rich domains that link membrane receptors to intracellular signaling proteins. For example, in a cell- and context-specific manner, the pTyr residues on GABs mediate binding of PI3K, the tyrosine phosphatase SHP2, phospholipase Cγ, and GRB2. It is Tyr^{452} on GAB2, one of three pTyr residues that mediates the binding of PI3K to GAB2 (35), that is dephosphorylated in response to FSH. GAB2 is most abundantly expressed in the ovary (36). Although deletion of GAB1 is embryonically lethal (37), GAB2 null mice are fertile (38, 39), perhaps because GAB1, which is also highly expressed in ovaries (36), can compensate for GAB2 (17).

GAB2 in GCs is a selective type I PKA AKAP that binds RIα. PKA is a tetrameric enzyme consisting of an R-subunit homodimer (RIα, RIβ, RIIα, and RIIβ that define PKA as type I or II) and two catalytic subunits. PKA activation is characterized by dissociation of the catalytic subunits on cAMP binding to the R-subunit dimer. Preantral GCs express only RIα and RIIα (30, 40). PKA holoenzymes are tethered to AKAPs that function to localize PKA substrates, phosphatases, and cAMP-phosphodiesterases to specific cellular locations to facilitate substrate phosphorylation in a spatiotemporal manner (41). Although the majority of AKAPs bind type II PKA, some have dual specificity and bind RI and RII, whereas a few selectively bind RI (32). PKA anchoring to AKAPs is mediated by an amphipathic helix of 14–18 aa on the AKAP that binds the R-subunit dimer (42). GAB2 contains a putative amphipathic helix (residues 218–232) that can be aligned with other known RI binding AKAPs (Fig. S8). GAB2 possesses position-specific hydrophobic residues (identified with asterisks) that fit with size restrictions, which were determined by structural (43) and mutation analyses (44), plus several charged (Asp^{221}and Lys$^{219,\ 226}$) and polar (Gln$^{218,\ 225,\ 229}$) residues that are commonly found interspersed between the hydrophobic residues. The ability of Ht31, the prototypical anchoring disruptor peptide that displaces both RI and RII (45), as well as the RI-selective peptide RIAD (32) to significantly reduce FSH-stimulated AKT(Ser^{473}) phosphorylation ($P < 0.05$ relative to control peptides) indicates that PKA signaling to PI3K is dependent on an RI AKAP. The more efficacious nature of Ht31 vs. RIAD to reduce AKT(Ser^{473}) phosphorylation, despite the higher affinity of RIAD for RI vs. RII (32), likely reflects the greater ability of the stearated Ht31 peptide to enter and/or its greater stability in GCs.

PKA guides the phosphorylation of IRS-1 on Tyr^{989} and dephosphorylation of GAB2 on Tyr^{452}. Future studies should identify relevant tyrosine phosphatase(s) and kinase(s) regulated by PKA that mediate these events. PKA directly phosphorylates GAB2 on Ser^{159}. In the MCF-7 breast cancer cell line, AKT

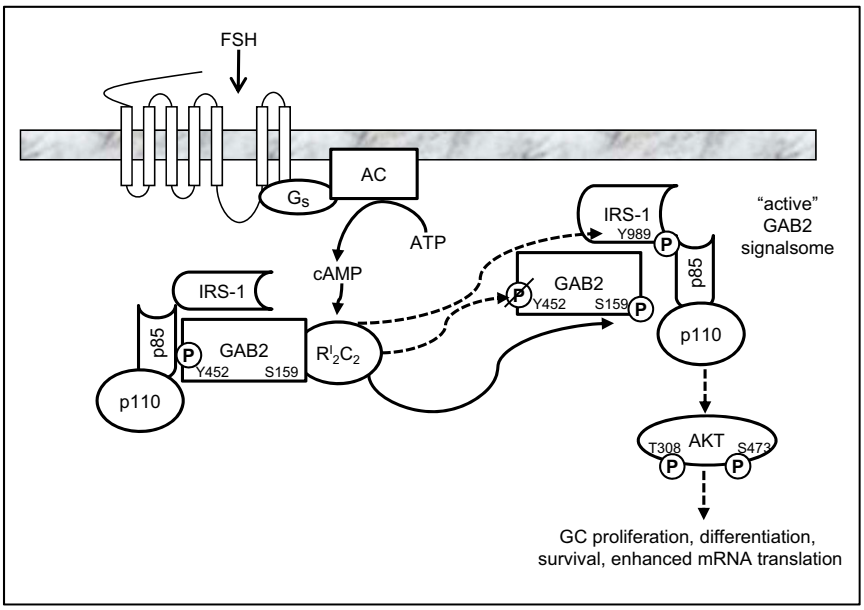

Fig. 7. Model of the signaling pathway by which FSH promotes AKT activation in GCs. FSH binding to and activation of the FSH GPCR leads to activation of the stimulatory G protein (G_s), activation of adenylyl cyclase (AC), generation of cAMP, and activation of the type I PKA holoenzyme ($R^I_2C_2$). PKA directly (unbroken line) or indirectly (broken line) promotes dephosphorylation (slash-P) of GAB2(Tyr^{452}) and phosphorylation (P) of GAB2(Ser^{159}) and IRS-1(Tyr^{989}). Phosphorylation of IRS-1 on Tyr^{989} provides the binding site for the p85 R-subunit of PI3K to allosterically activate the p110 catalytic subunit, resulting in phosphorylation-dependent activation of AKT(Thr^{308})(Ser^{473}) that promotes GC proliferation and differentiation.

phosphorylates GAB2 on Ser^{159} (46) and potentially sustains phosphorylation of this site in GCs, evidenced by preliminary results showing that wortmannin inhibits GAB2(Ser^{159}) phosphorylation (>50%) 60 min post-FSH but does not inhibit 10 min post-FSH (n = 2). GAB2 phosphorylated on Ser^{159} is associated with what we hypothesize to be an active GAB2 signalsome (Fig. 7). This hypothesis is based on the ability of p-GAB2(Ser^{159}) to coimmunoprecipitate with IRS-1 (Fig. 6*D*), the ability of p85 to readily pull down GAB2 in FSH-treated cells (Fig. 4*B*), the majority of which is phosphorylated on Ser^{159} (Fig. 6*D* and Fig. S7), the ability of p85 to readily pull down p-GAB2 (Ser^{159}) (Fig. 6*E*), and the ability FSH to enrich IRS-1 immunoprecipitations with p85 and p110 PI3K subunits (Fig. 4*C*). Proof of the functional significance of GAB2(Ser^{159}) phosphorylation requires future studies using adenoviral GAB2 (Ser^{159}/Ala or Asp) mutants. Additional studies are also required to formally prove that the pool of IRS-1 complexed with p-GAB2(Ser^{159}) is actively signaling to activate PI3K.

In the absence of FSH, GAB2 is also complexed with IRS-1 and PI3K. It is unlikely that IRS-1 is binding directly to GAB2, because GAB2 does not contain the canonical NPXY motif present on RTKs (12); however, we cannot rule out the direct association of IRS-1 with an unidentified GAB2 binding domain. The indirect binding of IRS-1 to GAB2 through GRB2 is also unlikely, because GAB2 does not seem to bind GRB2 in GCs based on the inability of GRB2 to be depleted from unbound fractions on GAB2 immunoprecipitation (Fig. S4*A*). We, thus, predict that the GAB2 signalsome contains at least one additional protein that links IRS-1 to GAB2. In contrast to IRS-1, PI3K likely binds directly to GAB2 through Tyr^{452} [Y^{441}VPM (homologous rat sequence)] in untreated GCs. The absence of detectable AKT phosphorylation in vehicle-treated GCs suggests that the apparent binding of the PI3K R-subunit to p-GAB2 (Tyr^{452}) is not sufficient to activate PI3K, perhaps because only a single p-YXXM motif is engaged (14). Rather, our results suggest that GAB2 constitutes a docking site for PI3K in vehicle-treated GCs. We hypothesize that, in response to FSH, PI3K switches from GAB2 to IRS-1 with the dephosphorylation of GAB2(Tyr^{452}) and phosphorylation of IRS-1(Tyr^{989}). Although the presence of a preformed complex minimally consisting of GAB2, PI3K, and IRS-1 prevents our testing this premise, the ability of our positive control, IGF_1, to also promote dephosphorylation of GAB2(Tyr^{452}) indirectly supports our switch model. Formal proof that GAB2(Tyr^{452}) dephosphorylation is upstream and necessary for activation of PI3K requires future studies in which we selectively prevent the dephosphorylation of this site.

Recent epidemiological studies link elevated insulin and/or IGF_1 and thus, enhanced signaling into PI3K with increased tumor incidence (47). Consistent with a tumorigenic model, FSH-stimulated AKT activation promotes enhanced HIF-1 activity, leading to expression of VEGF (48) and cell survival (8). There is also a wealth of data linking GAB2 with tumorigenesis (reviewed in ref. 17). For example, GAB2 is overexpressed in a number of solid tumors and cell lines, and it is required for signaling by oncogenic fusion proteins, such as the BCR-ABL tyrosine kinase fusion protein, to drive chromic myeloid leukemia (reviewed in ref. 17). The fact that this pathway can also be activated by PKA to replicate conditions consistent with tumorigenesis, such as increased proliferation, inhibition of apoptosis, and increased HIF-1 activity, shows that extracellular ligands that activate PKA need to be considered as potentially tumorigenic, especially because ectopic GPCR expression is common to cancer cells (49).

In sum, we have identified a pathway by which FSH-stimulated PKA hijacks GAB2 and IRS-1 to activate the PI3K pathway in GCs, leading to enhanced proliferation, inhibition of apoptosis, enhanced translation, and activation of target genes with products that define the mature, preovulatory GC (3–9). Our results reveal a previously unknown function for GAB2 as a multifactorial adaptor downstream of a GPCR and PKA. GAB2 and IRS-1 can no longer be considered only as adaptors downstream of RTKs or non-RTKs, and they also must be recognized as crucial mediators of cross-talk integrating pathways regulated by PKA.

Materials and Methods

Materials. oFSH-19 was purchased from the National Hormone and Pituitary Agency of the National Institute of Diabetes and Digestive and Kidney Diseases. Recombinant human IGF_1 was purchased from Atlanta Biologicals. The following antibodies were purchased: antiphospho-AKT (Ser^{473}; rabbit), antiphospho-AKT (Thr^{308}, rabbit), anti-AKT (rabbit), antiphospho-(Tyr) p85 PI3K binding motif (rabbit), anti–IRS-1 (rabbit), anti-GRB2 (rabbit), antiphospho-GAB2 (Tyr^{452}; rabbit), antiphospho-GAB2 (Ser^{159}, rabbit), anti–p110-PI3K (rabbit), and phospho-PKA substrate ($RRXS^P/T^P$, rabbit) from Cell Signaling Technologies; anti-SHP2 (rabbit and mouse) and antiphospho–IRS-1 (Tyr^{989}, rabbit) from Santa Cruz Biotechnology; anti-GAB2 (rabbit), anti-p85, PI3K (rabbit) agarose conjugate, anti–IRS-1 (rabbit) agarose conjugate, antiphospho-CREB (Ser^{133}, clone 10E9 mouse), and anti–IRS-2 (rabbit) from Upstate Biotechnology/Millipore; anti-p85, PI3K (mouse), anti-RI subunit of PKA (mouse), and anti-PKA catalytic subunit (mouse) from BD Biosciences; and antiprotein phosphatase 1 catalytic subunit-α from Calbiochem/EMD. Chemicals and peptides were purchased from the following vendors: myristoylated PKI 14–22 amide, wortmannin, and 8-CPT-cAMP were from Calbiochem/EMD; 8-CPT-2′-O-Me-cAMP was from Biolog; pepstatin A, aprotinin, leupeptin, benzamidine, PMSF, soybean trypsin inhibitor, and recombinant bovine heart PKA catalytic subunit were from Sigma-Aldrich; antipain dihydrochloride, calpain inhibitor III, and E-64 were from Roche; and human fibronectin was from BD Biosciences. RIAD (LEQYANQLADQIIKEATEK-RRRRRRRRRR) and RSCR (IEKELAQQYQNADAITLEK-RRRRRRRRRR) peptides were purchased from Biomatik; sHt31 (*N*-stearate-DLIEEAASRIVDAVIEQVKAAGAY) and sHt31-P (*N*-stearate-DLIEEAASRPVDAVPEQVKAAGAY) peptides were purchased from Promega.

Animals. Sprague–Dawley rats (Charles River Laboratories) were either housed at Northwestern University or from a breeder colony (originally from Charles River Laboratories) maintained by the Animal Reproduction Core, Center for Reproductive Biology at Washington State University. Both animal care facilities are maintained in accordance with the *Guidelines for the Care and Use of Laboratory Animals* by protocols approved by the Northwestern University or Washington State University Animal Care and Use Committees, respectively.

GC Culture and Western Blotting. Immature female rats were primed with s.c. injections of 1.5 mg estradiol-17β (E) in 0.1 mL propylene glycol on days 21–23 to promote growth of preantral follicles. GCs were isolated by manually puncturing follicles with 27-gauge needles (50). For each independent experiment, GCs from 10 to 20 rats were plated on fibronectin-coated plastic dishes at a density of $\sim 1 \times 10^6$ cells/mL in DMEM/F12 serum-free medium supplemented with 1 nM E, 100 U/mL penicillin (P), and 100 μg/mL streptomycin (S; E/PS) and treated with indicated additions ~20 h after plating (51). Vehicle controls correspond to equivalent concentrations of treatment diluents. Treatments were terminated by aspirating medium and rinsing cells one time with PBS. For Western blotting, total cell extracts were collected by scraping cells in SDS sample buffer (52) followed by heat denaturation. Protein concentrations were controlled by plating identical cell numbers per plate in each experiment and then loading equal volumes of total cell extracts per gel lane; GCs do not proliferate under these culture conditions. Equal protein loading was confirmed by indicated loading controls. Proteins were separated by SDS/PAGE and transferred to Hybond C-extra nitrocellulose (Amersham Biosciences) (53). Blots were incubated with primary antibody overnight at 4 °C, and antigen–antibody complexes were detected by enhanced chemiluminescence. Western signals were scanned with an Epson 1640SU scanner and Adobe Photoshop CS2 version 9.0 software with minimal processing and quantitated with Quantity One software program (Biorad Laboratories). Densitometric signal for experimental values was divided by the signal for control protein load, and it was expressed either as fold activation/inhibition over vehicle controls or relative to the maximal signal. Results were analyzed by Microsoft Excel or GraphPad Prism; significance was determined by Student *t* test.

Immunoprecipitation. Posttreatment and PBS wash, $\sim 10^7$ GCs were scraped into 1.0 mL lysis buffer [50 mM Hepes, pH 7.0, 100 mM NaCl, 0.5% Nonidet P-40, 20 mM NaF, 2 mM $NaVO_3$, 2 mM $Na_4P_2O_7$, 5 mM EGTA, 5 mM EDTA, 20 mM benzamidine, 10 μg/mL calpain inhibitor III, 50 μg/mL antipain, 50 μg/mL soybean trypsin inhibitor, 10 μM isomethylbutylxanthine, Halt protease inhibitor mixture (1 mM 4-(2-aminoethyl) benzenesulfonyl fluoride hydrochloride, 0.8 μM aprotinin, 50 μM bestatin, 15 μM E-64, 20 μM leupeptin, 10 μM pepstatin; Thermo Fischer Scientific)]. Lysates were sonicated 1 min on ice and clarified by centrifugation at 10,000 × *g* at 4 °C for 5 min. After removing 0.03 mL for input, soluble cell extracts were precleared by incubation with rabbit or mouse preclearing matrix (ExactaCruz F or C, respectively, depending on immunoprecipitating antibody host) for 1 h at 4 °C and then incubated overnight at 4 °C on a rotator in the presence of indicated antibodies and protein A/G PLUS-agarose (Santa Cruz Biotechnology) or antibody–agarose and control IgG–agarose conjugates. Unbound protein in the flow through was collected and denatured in SDS sample buffer. Agarose beads were washed four times in buffer containing 20 mM Hepes, pH 7.0, 150 mM NaCl, 10% glycerol, and 0.1% Triton X-100. Bound proteins were eluted, denatured in SDS sample buffer, and subjected to PAGE and Western blotting, RI far Westerns, or RII overlay assays. Input (taken before preclearing) represents ~3%, and bound represents ~97% of total sample volume.

In Vitro Phosphorylation Assays. Washed immunoprecipitated pellets from untreated GCs were incubated for 1 h at room temperature in a final volume of 0.1 mL containing 50 mM Tris·HCl, pH 7.5, 10 μM ATP, 10 mM $MgCl_2$, and ~6 μg PKA catalytic subunit or water. Pellets were washed two times; bound proteins were subjected to SDS/PAGE as described in *Immunoprecipitation*.

RI Far Western and RII Overlay Assays. For RI far Western assays, samples were transferred from SDS/PAGE gels to Immobilon-P PVDF membrane (Millipore), the membrane was blocked for 2 h with 5% milk in TBS-Tween, and it was incubated overnight at 4 °C with 0.3 ng/mL purified RIα, washed, and then subjected to standard Western blotting with anti-RI antibody. For RII overlay assay, samples were transferred to Immobilon-FL membrane; membranes were blocked in Odyssey blocking buffer for 1 h, incubated overnight at 4 °C in Odyssey blocking buffer with 0.1% Tween 20 and 3.4 mg/mL AlexaFluor 680 labeled RIIα, washed, and scanned using the Odyssey infrared imaging system (Li-Cor Biosciences). Purified recombinant RIIα (31) was labeled with the AlexaFluor 680 protein labeling kit (Molecular Probes).

Adenoviral Transduction of GCs. Transduction with adenoviruses was performed as previously described (5). In short, GCs were plated in 35-mm plates at 1.5×10^6 cells/2 mL in DMEM/F12 (E/PS). After GCs were allowed to adhere to fibronectin for 4 h, they were treated with adenovirus. The next morning, the adenovirus was washed off with PBS, DMEM/F12 and E/PS were added, and cells were treated as indicated. Adenoviral optical particle unit (OPU) concentration per milliliter viral stock was calculated from the A260 OD, measured in triplicate in a viral stock aliquot, diluted in 1% SDS, and boiled for 4 min at 100°C using the Nanodrop ND-1000 Spectrophotometer (http://www.google.com/patents/US7316898). Results are expressed as OPU per cell and based on the number of GCs plated and the volume of virus added. The following adenoviruses were provided: PKI by Marco Conti (University of California, San Francisco, CA) (54), S17N RAS by Valina Dawson (John Hopkins University School of Medicine, Baltimore, MD) (55), and WT GAB2 by Barry I. Posner (McGill University, Montreal) (56).

ACKNOWLEDGMENTS. We thank additional members of the Hunzicker-Dunn laboratory for their technical and intellectual contributions. We thank John Nilson for his critical reading of the manuscript. This work was supported by National Institutes of Health Grants R01HD062053 (to M.E.H.-D.) and R03HD068668 (to D.W.C.) and a Merit Award from the Department of Veterans Affairs (to D.W.C.).

1. Hunzicker-Dunn M, Mayo KE (2006) Gonadotropin signaling in the ovary. *The Physiology of Reproduction* (Elsevier, Amsterdam), Vol 3, pp 569–614.
2. Sprengel R, Braun T, Nikolics K, Segaloff DL, Seeburg PH (1990) The testicular receptor for follicle stimulating hormone: Structure and functional expression of cloned cDNA. *Mol Endocrinol* 4(4):525–530.
3. Zeleznik AJ, Saxena D, Little-Ihrig L (2003) Protein kinase B is obligatory for follicle-stimulating hormone-induced granulosa cell differentiation. *Endocrinology* 144(9): 3985–3994.
4. Alam H, et al. (2004) Follicle-stimulating hormone activation of hypoxia-inducible factor-1 by the phosphatidylinositol 3-kinase/AKT/Ras homolog enriched in brain (Rheb)/mammalian target of rapamycin (mTOR) pathway is necessary for induction of select protein markers of follicular differentiation. *J Biol Chem* 279(19):19431–19440.
5. Park Y, et al. (2005) Induction of cyclin D2 in rat granulosa cells requires FSH-dependent relief from FOXO1 repression coupled with positive signals from Smad. *J Biol Chem* 280(10):9135–9148.
6. Richards JS, et al. (2002) Novel signaling pathways that control ovarian follicular development, ovulation, and luteinization. *Recent Prog Horm Res* 57:195–220.
7. Cunningham MA, Zhu Q, Unterman TG, Hammond JM (2003) Follicle-stimulating hormone promotes nuclear exclusion of the forkhead transcription factor FoxO1a via

phosphatidylinositol 3-kinase in porcine granulosa cells. *Endocrinology* 144(12): 5585–5594.
8. Wang XL, et al. (2012) Follicle-stimulating hormone regulates pro-apoptotic protein Bcl-2-interacting mediator of cell death-extra long (BimEL)-induced porcine granulosa cell apoptosis. *J Biol Chem* 287(13):10166–10177.
9. Liu Z, et al. (2009) FSH and FOXO1 regulate genes in the sterol/steroid and lipid biosynthetic pathways in granulosa cells. *Mol Endocrinol* 23(5):649–661.
10. Manning BD, Cantley LC (2007) AKT/PKB signaling: Navigating downstream. *Cell* 129 (7):1261–1274.
11. Vanhaesebroeck B, Alessi DR (2000) The PI3K-PDK1 connection: More than just a road to PKB. *Biochem J* 346(Pt 3):561–576.
12. White MF (2002) IRS proteins and the common path to diabetes. *Am J Physiol Endocrinol Metab* 283(3):E413–E422.
13. McGettrick AJ, Feener EP, Kahn CR (2005) Human insulin receptor substrate-1 (IRS-1) polymorphism G972R causes IRS-1 to associate with the insulin receptor and inhibit receptor autophosphorylation. *J Biol Chem* 280(8):6441–6446.
14. Rordorf-Nikolic T, Van Horn DJ, Chen D, White MF, Backer JM (1995) Regulation of phosphatidylinositol 3′-kinase by tyrosyl phosphoproteins. Full activation requires occupancy of both SH2 domains in the 85-kDa regulatory subunit. *J Biol Chem* 270(8): 3662–3666.
15. Liu Y, Rohrschneider LR (2002) The gift of Gab. *FEBS Lett* 515(1–3):1–7.
16. Nishida K, Hirano T (2003) The role of Gab family scaffolding adapter proteins in the signal transduction of cytokine and growth factor receptors. *Cancer Sci* 94(12): 1029–1033.
17. Wöhrle FU, Daly RJ, Brummer T (2009) Function, regulation and pathological roles of the Gab/DOS docking proteins. *Cell Commun Signal* 7:22.
18. Vanhaesebroeck B, Guillermet-Guibert J, Graupera M, Bilanges B (2010) The emerging mechanisms of isoform-specific PI3K signalling. *Nat Rev Mol Cell Biol* 11(5):329–341.
19. Ciullo I, Diez-Roux G, Di Domenico M, Migliaccio A, Avvedimento EV (2001) cAMP signaling selectively influences Ras effectors pathways. *Oncogene* 20(10):1186–1192.
20. De Gregorio G, et al. (2007) The p85 regulatory subunit of PI3K mediates TSH-cAMP-PKA growth and survival signals. *Oncogene* 26(14):2039–2047.
21. Torella D, et al. (2009) Differential regulation of vascular smooth muscle and endothelial cell proliferation in vitro and in vivo by cAMP/PKA-activated p85alphaPI3K. *Am J Physiol Heart Circ Physiol* 297(6):H2015–H2025.
22. de Rooij J, et al. (1998) Epac is a Rap1 guanine-nucleotide-exchange factor directly activated by cyclic AMP. *Nature* 396(6710):474–477.
23. Kawasaki H, et al. (1998) A family of cAMP-binding proteins that directly activate Rap1. *Science* 282(5397):2275–2279.
24. Enserink JM, et al. (2002) A novel Epac-specific cAMP analogue demonstrates independent regulation of Rap1 and ERK. *Nat Cell Biol* 4(11):901–906.
25. Cheng HC, et al. (1986) A potent synthetic peptide inhibitor of the cAMP-dependent protein kinase. *J Biol Chem* 261(3):989–992.
26. Bain J, et al. (2007) The selectivity of protein kinase inhibitors: A further update. *Biochem J* 408(3):297–315.
27. Montminy MR, Bilezikjian LM (1987) Binding of a nuclear protein to the cyclic-AMP response element of the somatostatin gene. *Nature* 328(6126):175–178.
28. Hunzicker-Dunn M, Maizels ET (2006) FSH signaling pathways in immature granulosa cells that regulate target gene expression: Branching out from protein kinase A. *Cell Signal* 18(9):1351–1359.
29. Escamilla-Hernandez R, et al. (2008) Constitutively active protein kinase A qualitatively mimics the effects of follicle-stimulating hormone on granulosa cell differentiation. *Mol Endocrinol* 22(8):1842–1852.
30. Carr DW, et al. (1999) Identification of cAMP-dependent protein kinase holoenzymes in preantral- and preovulatory-follicle-enriched ovaries, and their association with A-kinase-anchoring proteins. *Biochem J* 344(Pt 2):613–623.
31. Carr DW, Scott JD (1992) Blotting and band-shifting: Techniques for studying protein-protein interactions. *Trends Biochem Sci* 17(7):246–249.
32. Carlson CR, et al. (2006) Delineation of type I protein kinase A-selective signaling events using an RI anchoring disruptor. *J Biol Chem* 281(30):21535–21545.
33. Pearce LR, Komander D, Alessi DR (2010) The nuts and bolts of AGC protein kinases. *Nat Rev Mol Cell Biol* 11(1):9–22.
34. Burks DJ, et al. (2000) IRS-2 pathways integrate female reproduction and energy homeostasis. *Nature* 407(6802):377–382.
35. Gu H, et al. (2000) New role for Shc in activation of the phosphatidylinositol 3-kinase/Akt pathway. *Mol Cell Biol* 20(19):7109–7120.
36. Nishida K, et al. (1999) Gab-family adapter proteins act downstream of cytokine and growth factor receptors and T- and B-cell antigen receptors. *Blood* 93(6):1809–1816.
37. Itoh M, et al. (2000) Role of Gab1 in heart, placenta, and skin development and growth factor- and cytokine-induced extracellular signal-regulated kinase mitogen-activated protein kinase activation. *Mol Cell Biol* 20(10):3695–3704.
38. Nishida K, et al. (2002) Requirement of Gab2 for mast cell development and KitL/c-Kit signaling. *Blood* 99(5):1866–1869.
39. Gu H, et al. (2001) Essential role for Gab2 in the allergic response. *Nature* 412(6843): 186–190.
40. DeManno DA, Jackiw V, Brooks EJ, Hunzicker-Dunn M (1994) Characterization of recombinant RI beta and evaluation of the presence of RI beta protein in rat brain and testicular extracts. *Biochim Biophys Acta* 1222(3):501–510.
41. Beene DL, Scott JD (2007) A-kinase anchoring proteins take shape. *Curr Opin Cell Biol* 19(2):192–198.
42. Carr DW, et al. (1991) Interaction of the regulatory subunit (RII) of cAMP-dependent protein kinase with RII-anchoring proteins occurs through an amphipathic helix binding motif. *J Biol Chem* 266(22):14188–14192.
43. Sarma GN, et al. (2010) Structure of D-AKAP2:PKA RI complex: Insights into AKAP specificity and selectivity. *Structure* 18(2):155–166.
44. Miki K, Eddy EM (1999) Single amino acids determine specificity of binding of protein kinase A regulatory subunits by protein kinase A anchoring proteins. *J Biol Chem* 274 (41):29057–29062.
45. Carr DW, Hausken ZE, Fraser ID, Stofko-Hahn RE, Scott JD (1992) Association of the type II cAMP-dependent protein kinase with a human thyroid RII-anchoring protein. Cloning and characterization of the RII-binding domain. *J Biol Chem* 267(19): 13376–13382.
46. Lynch DK, Daly RJ (2002) PKB-mediated negative feedback tightly regulates mitogenic signalling via Gab2. *EMBO J* 21(1-2):72–82.
47. LeRoith D (2010) Can endogenous hyperinsulinaemia explain the increased risk of cancer development and mortality in type 2 diabetes: Evidence from mouse models. *Diabetes Metab Res Rev* 26(8):599–601.
48. Alam H, et al. (2009) Role of the phosphatidylinositol-3-kinase and extracellular regulated kinase pathways in the induction of hypoxia-inducible factor (HIF)-1 activity and the HIF-1 target vascular endothelial growth factor in ovarian granulosa cells in response to follicle-stimulating hormone. *Endocrinology* 150(2):915–928.
49. Dorsam RT, Gutkind JS (2007) G-protein-coupled receptors and cancer. *Nat Rev Cancer* 7(2):79–94.
50. Carr DW, DeManno DA, Atwood A, Hunzicker-Dunn M, Scott JD (1993) Follicle-stimulating hormone regulation of A-kinase anchoring proteins in granulosa cells. *J Biol Chem* 268(28):20729–20732.
51. DeManno DA, et al. (1999) Follicle-stimulating hormone promotes histone H3 phosphorylation on serine-10. *Mol Endocrinol* 13(1):91–105.
52. Hunzicker-Dunn M (1981) Selective activation of rabbit ovarian protein kinase isozymes in rabbit ovarian follicles and corpora lutea. *J Biol Chem* 256(23):12185–12193.
53. Salvador LM, et al. (2001) Follicle-stimulating hormone stimulates protein kinase A-mediated histone H3 phosphorylation and acetylation leading to select gene activation in ovarian granulosa cells. *J Biol Chem* 276(43):40146–40155.
54. Bruss MD, Richter W, Horner K, Jin SL, Conti M (2008) Critical role of PDE4D in beta2-adrenoceptor-dependent cAMP signaling in mouse embryonic fibroblasts. *J Biol Chem* 283(33):22430–22442.
55. Gonzalez-Zulueta M, et al. (2000) Requirement for nitric oxide activation of p21(ras)/extracellular regulated kinase in neuronal ischemic preconditioning. *Proc Natl Acad Sci USA* 97(1):436–441.
56. Kong M, Mounier C, Wu J, Posner BI (2000) Epidermal growth factor-induced phosphatidylinositol 3-kinase activation and DNA synthesis. Identification of Grb2-associated binder 2 as the major mediator in rat hepatocytes. *J Biol Chem* 275(46): 36035–36042.